PERGAMON

International Journal of Heat and Mass Transfer 42 (1999) 4197–4205

International Journal of HEAT and MASS TRANSFER

www.elsevier.com/locate/ijhmt

# Melting of unfixed material in spherical capsule with non-isothermal wall

S.A. Fomin[a], T.S. Saitoh[b,*]

[a]*Kazan State University, PO Box 382, 420503 Kazan, Russia*
[b]*Department of Aeronautics and Space Engineering, Tohoku University, Sendai 980-8579, Japan*

Received 15 July 1998; received in revised form 9 February 1999

**Abstract**

Close-contact melting within a spherical capsule is investigated both numerically and analytically. A complete mathematical model is solved numerically by utilizing the boundary fixing method. The approximate approach developed by Bareiss and Beer for the horizontal cylinder is applied to constructing an approximate mathematical model of contact melting in a spherical capsule with a non-isothermal wall. The main characteristic scales and dimensionless parameters which describe the principal features of the melting process are found. Due to the presence of the small parameter in governing equations the perturbation method is implemented. As a result, simple analytical solutions were found which describe close-contact melting inside the capsule with a non-isothermal wall and account for the streamwise convection in the molten layer. The extensive validation of the analytical solution, and its comparison with the numerical results, gives the proof of accuracy of the analytical solutions with estimated error of 10–15%. This conclusion is of crucial importance for evaluating the real latent heat thermal energy storage systems which contain thousands of capsules, since the simple closed-form solutions for a single capsule, used in the mathematical modeling of such kind of complex systems, significantly reduces the cost of numerical computations. 

## 1. Introduction

The analysis of close-contact melting of a solid in cavities is motivated by application in latent heat-of-fusion thermal storage systems. This phenomenon was studied by inclusion of density change during melting of unconfined solids in horizontal cylindrical capsule, numerically by Saitoh and Hirose [1], experimentally by Katayama et al. [2], analytically and experimentally by Bareiss and Beer [3]. Contact melting in a spherical capsule was investigated numerically by Moore and Bayazitoglu [4], Hoshina and Saitoh [5] and later, by applying the technique proposed in [3], Bahrami and Wang [6] and Roy and Sengupta [7] reported analytical solutions. The general scheme for scale analysis of the contact melting problem was proposed by Bejan [8]. Although the aforementioned investigations highlight the main characteristics of contact melting in enclosure, the effect of temperature variation along the wall of the spherical capsule has not been analyzed, and the tangential force convection in the molten layer was neglected. Number of errors and confusing misprints in a recently published paper dealing with contact melting in non-isothermal cylindrical capsule [9] is so excessive that it makes practically impossible neither to use the presented result nor to estimate its correctness. His phrase that 'the time scale of this change is

* Corresponding author. Tel.: +81-22-217-6974; fax: +81-22-217-6975.
*E-mail address:* saitoh@cc.mech.tohoku.ac.jp (T.S. Saitoh)

0017-9310/99/$ - see front matter 
PII: S0017-9310(99)00080-0

**Nomenclature**

| | |
|---|---|
| $A$ | parameter defined in Eqs. (24) and (25) |
| $Ar$ | Archimedes number $=\rho_l g R^3(\rho_s-\rho_l)/\mu^2$ |
| $a$ | coefficient in capsule's wall temperature equation $T_w=1+a\sin^2\theta$ |
| $B$ | parameter defined in Eqs. (24) and (25) |
| $C_\delta$ | molten layer thickness scale to capsules radius ratio $=\delta_0/R$ |
| $C_\rho$ | solid-to-liquid density ratio $=\theta_s/\theta_l$ |
| $c_l$ | liquid specific heat |
| $f_1, f_2$ | functions determined in Eq. (23) |
| $g$ | gravitational acceleration |
| $h_m$ | latent heat of melting |
| $k_l$ | thermal conductivity of liquid |
| $M$ | molten mass |
| $M_{tot}$ | total molten mass |
| $Pr$ | Prandtl number $=c_l\mu/k_l$ |
| $p$ | liquid pressure |
| $\bar{p}$ | surplus liquid pressure $=p-3(\cos\theta+1)/4(C_\rho-1)$ |
| $p_0$ | characteristic pressure determined in Eq. (6) |
| $q_w$ | heat flux on wall of capsule |
| $q_m$ | heat flux on the melting solid–liquid interface |
| $R$ | radius of capsule |
| $r$ | polar coordinate, as in Fig. 1 |
| $s$ | shift of reference point fixed in solid core |
| $Ste$ | Stefan number $=c_l(T_{w0}-T_m)/h_m$ |
| $T$ | dimensionless liquid temperature determined in Eq. (5) |
| $T_l$ | dimensional liquid temperature |
| $T_m$ | melting point |
| $T_w$ | dimensionless wall temperature |
| $T_{w0}$ | reference wall temperature (temperature at the point $\theta=0$) |
| $u_0$ | scale for tangential velocity determined in Eq. (6) |
| $u_x$ | dimensionless transverse velocity determined in Eq. (5) |
| $u_\eta$ | dimensional tangential velocity determined in Eq. (5) |
| $x$ | dimensionless variable $=(R-r)/\delta_0$ |

*Greek symbols*

| | |
|---|---|
| $\alpha$ | thermal diffusivity of liquid |
| $\delta$ | dimensionless molten layer thickness |
| $\delta_0$ | scale for molten layer thickness determined in Eqs. (6) |
| $\theta$ | polar angle, as shown in Fig. 1 |
| $\theta_a$ | polar angle which indicates contact melting area, as shown in Fig. 1 |
| $\mu$ | dynamic viscosity |
| $\rho_l$ | density of liquid |
| $\rho_s$ | density of solid |
| $\tau$ | dimensionless time |
| $\tau_0$ | time scale as determined in Eq. (6) |
| $\tau_m$ | time required to complete melting of solid core |

*Superscript*

| | |
|---|---|
| * | dimensional quantity |

*Subscripts*

| | |
|---|---|
| l | liquid |
| m | melting |
| s | solid |
| w | wall of the capsule |

small compared with the heat transfer rate and liquid flow rate' is very confusing and unclear, and no estimations have been provided. The comparison with the previous results for contact melting in a cylindrical enclosure also was not provided.

In the present paper the excellent approximate approach developed by Bareiss and Beer [3] is applied for the mathematical modeling of contact melting in the spherical capsule with non-isothermal wall. The latter condition was motivated by our experiments for the real thermal energy storage systems. The results of the experiments indicate that isothermal wall of the capsule never exists in practice. Since the temperature overfall along the cavity wall may cause the substantial temperature gradient in the molten layer in the tangential direction, therefore, the convective term in the energy equation is preserved in our model.

## 2. System model and analysis

A schematic sketch of melting process within a spherical enclosure is illustrated in Fig. 1. A sphere of the radius $R$ containing phase-change material initially is in the solid phase and entirely at melting point $T_m$. The wall temperature is instantly raised to temperature $T_w$ which is higher than $T_m$. As a result, inward melting of the solid starts. Owing to its higher density the unfixed solid bulk acquires vertically downward speed. The downward motion of the solid core is character-

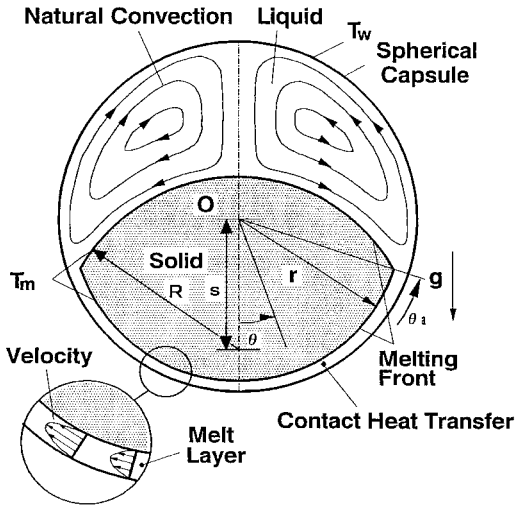


Fig. 1. A schematic sketch of close-contact melting in a spherical capsule.

ized by the time-dependent shift of a material-fixed reference point, which is chosen to be the center of the originally, spherical core. The motion of the solid bulk is accompanied by generation of liquid at the melting interface and the liquid is squeezed up through a narrow gap between the melting surface and the wall of the capsule, to the space above the solid. Conventionally, the solid-liquid interface can be divided into two parts as denoted in Fig. 1 by the time dependent value of the polar angle $\theta_a$: a bottom interface ($\theta \leqq \theta_a$) which represents the close-contact melting area where the most intensive melting occurs, and the upper interface where much slower 'latent' melting takes place.

The complete mathematical model of the combined close-contact and natural convection melting inside a spherical capsule is presented in [5]. The results obtained in this study show that the melting process exhibits an unsteady behavior only over the first few seconds from the beginning of melting. It was revealed that melting at the upper solid surface was approximately 10–15% of total melt. Moreover, the shape of the upper interface does not change and can be well approximated by a circular arc with invariable curvature throughout the entire process. The latter was also proved experimentally by Bareiss and Beer [3] who considered melting in a horizontal capsule. It was discovered by the aforementioned investigations that the thickness of the molten layer $\delta$ in the close-contact area is considerably smaller than the capsule radius $R$. On the basis of these conclusions, the primary assumptions made in the present study are the following:

1. Melting at the upper surface of the solid core is negligibly small [3,5].
2. The process is quasi-steady. Therefore, the acting forces are balanced, when the vertical resultant of the pressure force in the liquid layer between the bottom interface and the heated wall of the capsule, is equal to the value of the difference between the gravitational and buoyancy forces of the solid bulk. The velocity profile in the liquid film is also quasi-steady and changes only with the film thickness which varies with time.
3. The flow in the capsule is axisymmetric around the vertical axis of the sphere and two-dimensional spherical polar coordinate system ($r$, $\theta$) can be employed.
4. Since the thickness of the liquid layer in the close-contact area is very small relative to the dimension of the sphere, the lubrication theory approach can be implemented for mathematical modeling of heat and mass transfer processes at the bottom of the capsule.

### 2.1. Governing equations

After the proper scale analysis of the complete mathematical model of melting process inside the capsule, presented for instance in [5], the main characteristic scales and dimensionless parameters which describe the principal features of the melting process, were found. Among the most important values to be mentioned is a parameter

$$C_\delta = \left[\frac{3\alpha\mu Ste}{4R^3 g(\rho_s - \rho_l)}\right]^{1/4}$$

which represents [5] the ratio of the characteristic scale for the molten layer thickness to the radius $R$ of the capsule. Parameter $C_\delta$ varies in the range of $10^{-3}$–$10^{-2}$ for different phase change materials used in thermal storage systems. Accounting for the presence of this small parameter, the model was simplified by neglecting the terms of the order $O(C_\delta)$. By the proper non-dimensionalizing of the momentum and energy equations and boundary conditions, a small parameter $C_\delta$ has appeared as a coefficient in front of some terms of these equations. The terms which are multiplied to this parameter have the order of $O(C_\delta)$ and can be considered as neglectfully small and omitted in comparison with those ones that have order of $O(1)$ and are refined in the equations. For instance the inertial terms in the momentum equation in theta direction have the order of $O(C_\delta)$ and therefore neglected in the viscous part of this equation the derivative of $u$ with respect to theta of the second order has the higher degree of smallness and has multiplicity of $C_\delta^2$ and also neglected. In the momentum equation in $r$-direction all

the terms except the pressure have the multiplicity of $C_\delta$ or more high degree of smallness that is why they are omitted. In the energy equation the dissipative part has the multiplicity of $C_\delta$ and therefore neglected, due to the same reasons the second order derivative of temperature with respect to theta is also omitted. As a result, the dimensionless mass conservation, momentum and energy equations governing heat and mass transfers in a molten layer under the solid bulk pressed by its own weight to the capsule wall, are converted to the following form:

$$\frac{\partial u_x}{\partial x} + \frac{1}{\sin\ \theta}\ \frac{\partial}{\partial \theta}(u_\theta\ \sin\ \theta) = 0 \tag{1}$$

$$\frac{\partial p}{\partial \theta} = \frac{\partial^2 u_\theta}{\partial x^2} - \frac{3\ \sin\ \theta}{4(C_\rho - 1)} \tag{2}$$

$$Ste\left(u_x \frac{\partial T}{\partial x} + u_\theta \frac{\partial T}{\partial \theta}\right) = \frac{\partial^2 T}{\partial x^2} \tag{3}$$

The momentum equation in the $r$-direction reduces to $\partial p/\partial x = 0$, hence $p$ is a function of one independent variable $\theta$.

The dimensionless Stefan condition on the solid–liquid interface $x = \delta$ yields

$$\frac{\mathrm{d}s}{\mathrm{d}\tau}\cos\ \theta = -\left.\frac{\partial T}{\partial x}\right|_{x=\delta}. \tag{4}$$

The dimensionless variables in Eqs. (1)–(4) are chosen as follows:

$$\begin{aligned} &u_x = \frac{\tau_0 u*_x}{2RC_\rho}, \quad u_\theta = \frac{u*_\theta}{u_0}, \quad \delta = \frac{\delta*}{\delta_0}, \quad \tau = \frac{\tau*}{\tau_0}, \\ &s = \frac{s*}{2R}, \quad x = \frac{R-r}{\delta_0}, \quad T = \frac{T_1 - T_\mathrm{m}}{T_{\mathrm{w}0} - T_\mathrm{m}}, \\ &p = \frac{p*}{p_0}, \end{aligned} \tag{5}$$

where $\tau_0$, $u_0$, $p_0$ and $\delta_0$, are the initially unknown scales for time of melting, tangential velocity, pressure, and thickness of the molten layer, respectively. These values found over the scale analysis are

$$\begin{aligned} &\tau_0 = \frac{2R^2 C_\delta C_\rho}{\alpha Ste}, \quad u_0 = \frac{\alpha Ste}{RC_\delta^2}, \quad \delta_0^4 = \frac{3R^4 Ste}{4ArPr}, \\ &p_0 = \frac{4}{3}Rg(\rho_\mathrm{s} - \rho_\mathrm{l}), \end{aligned} \tag{6}$$

where

$$\begin{aligned} &C_\rho = \rho_\mathrm{s}/\rho_\mathrm{l}, \quad Ar = \rho_\mathrm{l} g R^3(\rho_\mathrm{s} - \rho_\mathrm{l})/\mu^2, \\ &Pr = c_\mathrm{l}\mu/k_\mathrm{l}. \end{aligned} \tag{7}$$

Nondimensional equation of the force balance [7] between the load exerted by the solid core bounded by spherical surfaces on the thin liquid layer and stresses in this layer with an accuracy of $O(C_\delta)$ is

$$\begin{aligned} 2\int_0^{\theta_\mathrm{a}} &p \sin\theta\cos\theta\,\mathrm{d}\theta \\ &= 1 - \frac{3}{2}s + \frac{s^3}{2} + \frac{3}{2(C_\rho - 1)}\int_0^{\theta_\mathrm{a}} (1 + \cos\theta)\sin\theta \\ &\cos\theta\,\mathrm{d}\theta, \end{aligned} \tag{8}$$

where at the exit point of the close-contact area

$$p(\theta_\mathrm{a}) = \frac{3(1 + \cos\ \theta_\mathrm{a})}{4(C_\rho - 1)}.$$

### 2.2. Analytical solution

Integrating Eq. (2) twice with respect to $x$ and accounting for no-slip conditions on the both solid wall and lower melting interface, gives

$$u_\theta = \frac{1}{2}\ \frac{\mathrm{d}\bar{p}}{\mathrm{d}\theta} x(x - \delta), \tag{9}$$

where

$$\bar{p} = p - \frac{3\ \cos\ \theta}{4(C_\rho - 1)}.$$

Integration of Eq. (1) over the interval $(0, \delta)$ provides a formula for the pressure gradient in the liquid as

$$\frac{\mathrm{d}\bar{p}}{\mathrm{d}\theta} = -\frac{6\ \sin\ \theta}{\delta^3}\ \frac{\mathrm{d}s}{\mathrm{d}\tau}. \tag{10}$$

Combining Eqs. (9) and (10), the velocity distribution in the molten layer can be rewritten as follows

$$u_\theta = \frac{3\ \sin\ \theta}{\delta}\ \frac{\mathrm{d}s}{\mathrm{d}\tau}\left(\frac{x}{\delta}\right)\left(1 - \frac{x}{\delta}\right). \tag{11}$$

Integrating the energy Eq. (3) across the molten layer $(0, \delta)$ and using the mass conservation Eq. (1), the following heat balance integral equation is obtained

$$\frac{Ste}{\sin\ \theta}\ \frac{\partial}{\partial \theta}\left(\int_0^\delta u_\theta T\ \sin\ \theta\,\mathrm{d}x\right) = q_\mathrm{w} - q_\mathrm{m}, \tag{12}$$

where $q_\mathrm{w}$ and $q_\mathrm{m}$ are heat fluxes on the capsule wall and melting surface, respectively. Approximating the temperature profile in the molten layer by the third-

order polynomial and imposing the obvious boundary conditions on the wall of the enclosure

$$x=0,\quad T=T_{\mathrm{w}},\quad \frac{\partial^2 T}{\partial x^2}=0 \tag{13}$$

and on the solid–liquid interface

$$x=\delta,\quad T=0,\quad \frac{\partial T}{\partial x}=-\cos\ \theta\frac{\mathrm{d}s}{\mathrm{d}\tau} \tag{14}$$

leads to

$$T=\frac{T_{\mathrm{w}}}{2}\left(2-3\left(\frac{x}{\delta}\right)+\left(\frac{x}{\delta}\right)^3\right)+\frac{\delta}{2}\frac{\mathrm{d}s}{\mathrm{d}\tau}\cos\theta\left(1-\left(\frac{x}{\delta}\right)^2\right)\left(\frac{x}{\delta}\right). \tag{15}$$

Substituting the formulae (11) and (15) into Eq. (12) gives a differential equation for the unknown thickness of the molten layer $\delta=\delta(\theta)$

$$\frac{Ste\delta}{60\sin\theta}\frac{\mathrm{d}s}{\mathrm{d}\tau}\frac{\mathrm{d}}{\mathrm{d}\theta}\left[\sin^2\theta\left(7T_{\mathrm{w}}+3\delta\frac{\mathrm{d}s}{\mathrm{d}\tau}\cos\theta\right)\right]=T_{\mathrm{w}}-\delta\frac{\mathrm{d}s}{\mathrm{d}\tau}\cos\theta. \tag{16}$$

As was already mentioned, the derivation of the simplified mathematical model presented above is based on the fact that parameter $C_\delta=\delta_0/R\sim 10^{-3}-10^{-2}$ and therefore the values of $O(C_\delta)$ can be ignored. The simplified model has another small parameter; Stefan number. For all possible situations and variety of the phase change materials, $Ste<1$. The latter allows to implement the perturbations method.

Solution of Eq. (16) is sought in the form of an asymptotic series

$$\delta=\delta_1+\delta_2 Ste+\delta_3 Ste^2+\delta_4 Ste^3+\cdots. \tag{17}$$

Substituting series (17) into Eq. (16) and collecting the terms with parameter $Ste$ of the equal power leads to

$$(Ste)^0:\quad T_{\mathrm{w}}-\delta_1\frac{\mathrm{d}s}{\mathrm{d}\tau}\cos\ \theta=0, \tag{18}$$

$$(Ste)^1:\quad \frac{\delta_1}{60\sin\theta}\frac{\mathrm{d}}{\mathrm{d}\theta}\left[\sin^2\theta\left(7T_{\mathrm{w}}+3\delta_1\frac{\mathrm{d}s}{\mathrm{d}\theta}\cos\theta\right)\right]=-\delta_2\cos\theta. \tag{19}$$

More bulky equations for $\delta_3$, $\delta_4$, $\delta_5$, etc., which also can be readily obtained, are not presented here since the Stefan number is very small and in the majority of applications, the second order approximation is quite sufficient for the further analysis. Therefore, using Eqs. (18) and (19), the series (17) leads to the following approximate correlation:

$$\delta=\frac{T_{\mathrm{w}}}{\frac{\mathrm{d}s}{\mathrm{d}\tau}\cos\theta}\left[1-\frac{Ste}{3\sin 2\theta}\frac{\mathrm{d}}{\mathrm{d}\theta}(\sin^2\theta T_{\mathrm{w}})+O(Ste^2)\right]. \tag{20}$$

Substituting $\delta$, defined by Eq. (20), into Eq. (10) and neglecting the terms of $O(Ste^2)$, yields

$$\frac{\mathrm{d}\bar{p}}{\mathrm{d}\theta}=-\frac{6\sin\theta\cos^3\theta}{T_{\mathrm{w}}^3}\left(\frac{\mathrm{d}s}{\mathrm{d}\tau}\right)^4\left[1+\frac{Ste}{\sin 2\theta}\frac{\mathrm{d}}{\mathrm{d}\theta}(\sin^2\theta T_{\mathrm{w}})\right]. \tag{21}$$

With regard to this equation and using the kinematic relationship; $\cos\ \theta_{\mathrm{a}}=s$, an expression for the downward velocity of the solid bulk $\mathrm{d}s/\mathrm{d}\tau$ can be derived from the force balance Eq. (8) as follows:

$$\left(\frac{\mathrm{d}s}{\mathrm{d}\tau}\right)^4=\frac{\frac{4}{3}\left(1-\frac{3}{2}s+\frac{s^3}{2}\right)}{\int_0^{\arccos s}\frac{\sin^3 2\theta}{T_{\mathrm{w}}^3}\left[1+\frac{Ste}{\sin\ 2\theta}\frac{\mathrm{d}}{\mathrm{d}\theta}(\sin^2\theta T_{\mathrm{w}})\right]\mathrm{d}\theta}. \tag{22}$$

According to our measurements [10] the wall temperature distribution $T_{\mathrm{w}}$ can be estimated by $T_{\mathrm{w}}=1+a\sin^2\theta$, where $0\le\theta\le\theta_{\mathrm{a}}\le\pi/2$ and parameter $a$ is selected from the experiment. In that experiment it was found that parameter $a$ may vary from 0 to 0.4 and can be approximately chosen as 0.2. In this paper we vary the parameter $a$ in order to investigate how the distribution of the wall's temperature influences the melting process. Based on the data provided in [10] parameter $a$ (is approximately equal to) 0.2. In this case the integral in the right-hand side of the Eq. (22) can be expressed as elementary functions and Eq. (22) leads to

$$\frac{\mathrm{d}s}{\mathrm{d}\tau}=\left\{\frac{1-3s/2+s^3/2}{6[f_1(s)+(f_1(s)+af_2(s))Ste]}\right\}^{1/4}, \tag{23}$$

where

$$f_1=\frac{1}{2a^2}\left[\frac{(1-s^2)(2+a(a+3)(1-s^2))}{2[1+a(1-s^2)]^2}-\frac{\ln[1+a(1-s^2)]}{a}\right],$$

$$f_2 = \frac{1}{2a^3}\left[\frac{(s^2-1)(6+11a+5a^2-9as^2-7a^2s^2+2a^2s^4)}{[1+a(1-s^2)]^2} + \frac{2(3+a)\ln[1+a(1-s^2)]}{a}\right].$$

Substituting these analytical expressions for the dimensionless melting rate into Eqs. (11), (15), (20) and (21), leads to the closed-form solutions for the dimensionless molten layer velocity, temperature, thickness and pressure gradient, respectively.

In order to obtain a simple, but nevertheless accurate analytical solution of Eq. (23), and to express the melting time in the elementary functions, the inverse of the quantity in the right-hand side of Eq. (23) can be substituted with the vanishing error by a first-order polynomial $f(s)=a_1s+a_0$. The introduction of this approximate but adequate formula is based on the results provided by Bariess and Beer [3], Moallemi et al. [11], Bahrami and Wang [6] and Roy and Sengupta [7]. According to their results the parabolic polynomial is well fitted to the melting time curve $\tau=\tau(s)$, therefore, the linear profile can be chosen for its derivative $d\tau/ds$. The coefficients $a_1$ and $a_0$ can be obtained by using the values of the function $d\tau/ds=f(s)$ in the points $s=0$ and $s=1$. Taking the limits in Eq. (23) for $s\to 0$ and $s\to 1$ yields

$$\lim_{s\to 1} f(s) = \sqrt{2}(1+Ste/4)+O(Ste^2), \tag{24}$$

$$\lim_{s\to 0} f(s) = A+(A+B)Ste/4+O(Ste^2), \tag{25}$$

where

$$A=\left(\frac{3}{2a^3}\right)^{1/4}[a+a/(1+a)-2\ \ln(1+a)]^{1/4},$$

$$B=\left(\frac{24}{1+a}\right)^{1/4}\frac{-6a-5a^2+(6+8a+2a^2)\ln(1+a)}{[a(2a+a^2-2(1+a)\ln(1+a))]^{3/4}}.$$

Eqs. (24) and (25) lead to

$$\frac{d\tau}{ds} = [(\sqrt{2}-A)+(\sqrt{2}-A-B)Ste/4]s+A+(A+B)Ste/4. \tag{26}$$

Integration of Eq. (26) with the obvious boundary condition $s(0)=0$ results in

$$\tau = [(\sqrt{2}-A)+(\sqrt{2}-A-B)Ste/4]s^2/2+[A+(A+B)Ste/4]s. \tag{27}$$

The entire mass is molten when $s=1$ or $\tau_m=\tau(1)$

$$\tau_m = (\sqrt{2}+A)/2+(\sqrt{2}+A+B)Ste/8. \tag{28}$$

Dividing Eq. (27) by Eq. (28) leads to a useful relationship for $\tau/\tau_m$ which represents the fraction of time elapsed relative to the time required for complete melting, expressed in terms of the shift distance $s$ of the solid. Apparently, the value of the relative dimensionless time $\tau/\tau_m=1$ corresponds to the complete melting of the solid core.

In this particular case, when the Stefan number is very small, for instance $Ste<0.1$, the terms in the Eqs. (20)–(27), which are multiplied by $Ste$ can be neglected. Physically, it means that convection in the tangential direction is ignored. The latter assumption leads to the following simplified relationships for the thickness of the molten layer, melting rate and melting time, respectively;

$$\delta = T_w/\left(\frac{ds}{d\tau}\cos\ \theta\right), \tag{29}$$

$$\frac{ds}{d\tau} = \left(\frac{1-3s/2+s^3/2}{6f_1(s)}\right)^{1/4}, \tag{30}$$

$$\tau = (\sqrt{2}-A)s^2/2+As. \tag{31}$$

## 3. Results and discussion

Among the different phase change materials used in the thermal energy storage systems, *n*-octadecane is of most frequent use. Physical properties of this material are well documented and, for example, can be detected in [5–7]. Even though numerical computations provided below are for *n*-octadecane melting conditions, general conclusions can be drawn. The ratio of the characteristic thickness of the molten layer to the radius of the capsule is given by

$$C_\delta = \frac{\delta_0}{R} = \left(\frac{3Ste}{4ArPr}\right)^{1/4}.$$

The thickness of the molten layer therefore is decreased by reducing the viscosity and temperature difference $T_{w0}-T_m$, and by increasing of the density difference $\rho_s-\rho_l$, respectively. Since the phase change material in the capsule is chosen, in our case it is *n*-octadecane, the only controlling parameter is characteristic temperature of the wall $T_{w0}$ which affects the Stefan number. But even though the smaller Stefan numbers provide the decrease of the molten layer thickness, the dimensionless melting time which can be determined as

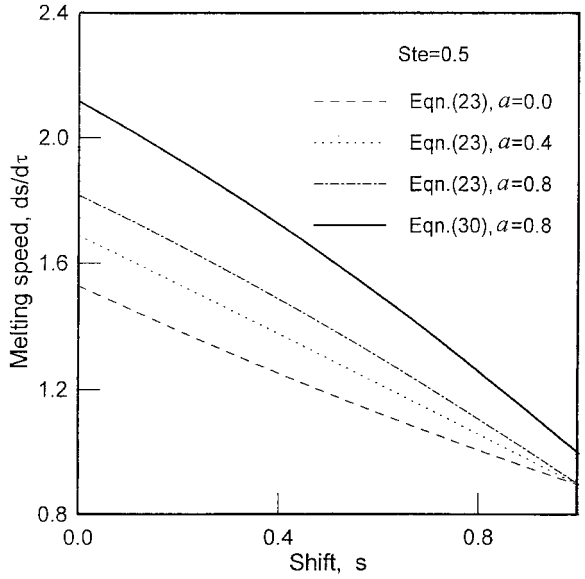


Fig. 2. Variation of the downward speed of solid $ds/d\tau$ with solid travel distance $s$.

$$Fo_0 = \frac{\tau_0 \alpha}{R^2} = \frac{2C_\rho}{Ste^{3/4}}\left(\frac{3}{4ArPr}\right)^{1/4}$$

will increase. On the contrary, the inverse quantity-the characteristic melting rate $2R/\tau_0$ increases with the increase of the Stefan number.

In order to study the influence of the temperature distribution $T_w$ along the wall of the capsule, a series of computations for different variations of temperature were carried out. Temperature on the wall was specified by equation $T_w = 1 + a \sin^2 \theta$, where the coefficient $a$ determines a temperature difference along the wall between the stagnation point $\theta = 0$ and the end point $\theta = \theta_a$ of the close-contact area. The analytical solutions for the dimensionless melting rate $ds/d\tau$ as a function of the solid core shift are presented in Fig. 2. The computed results illustrate the influence of the temperature distribution along the wall of the capsule. More stronger increase of the wall temperature ($a = 0.4$ or furthermore $a = 0.8$) leads to a higher melting speed. Solid line corresponds to the first order approximation when $\delta = \delta_1$ and the convective term in the energy equation is ignored. These computations based on Eq. (30) show that this rough approximation, which does not account for heat outflow from the molten layer, results in exaggeration of the melting speed. The similar conclusions can be made by inspecting Fig. 3 which presents the variation of the solid core travel distance with time elapsed. Curves 1, 2 and 3 indicate that the time required for melting the solid core is shorter if the temperature $T_w$, increases along the wall of the capsule. Ignoring the streamwise convection in the liquid (curves 1, 2 and 3) results in predicting of excessively high rates of melting.

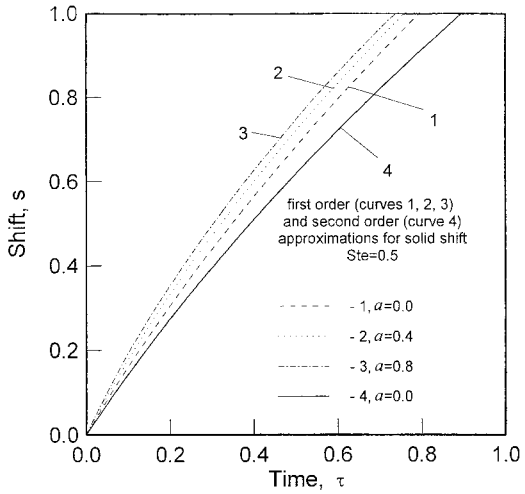


Fig. 3. Solid travel distance $s$ vs dimensionless time.

Assuming that the capsule wall is isothermal ($a = 0$) and heat transfer is dominated by heat conduction across the molten layer only, and therefore Eq. (31) is applicable, the comparison of the computed solid shift as a function of the relative time with the results of Bahrami and Wang [6] are provided. For these conditions solutions are completely coincidental, as shown in Fig. 4.

As it was mentioned above, experimental studies of melting within capsules indicate that around 85–90% of solid core is melted by close-contact melting with the heated wall at the bottom of the capsule, and the rest of the solid melts due to heat conduction and natural convection in the upper liquid region in the

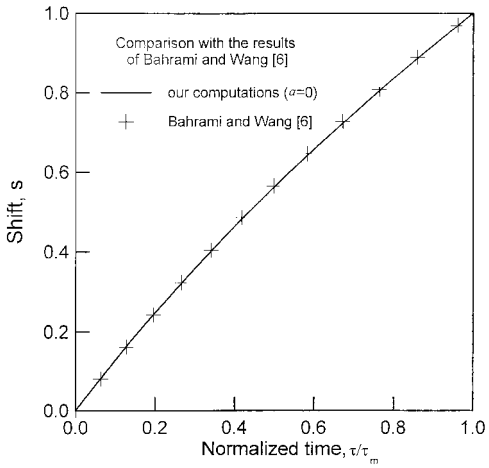


Fig. 4. Solid travel distance as a function of time elapsed relative to the time required for complete melting.

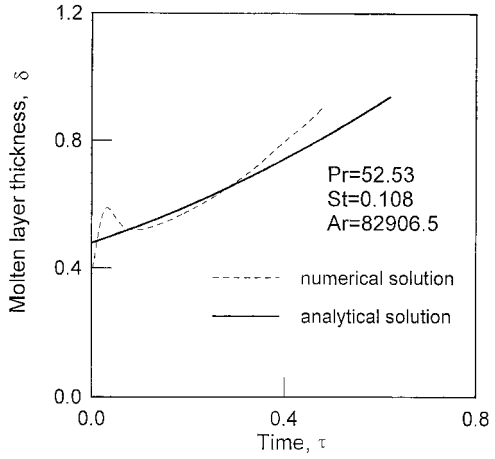


Fig. 5. Time history of the molten layer thickness at the bottom of the capsule ($\theta = 0$).

capsule. In order to estimate theoretically the melting process in the upper part of the capsule the complete mathematical model available for instance in [5] and [10] was solved numerically. The Boundary Fixing Method [12] was used to handle the moving interface between the liquid region and the solid region. Numerical results roughly agree with analytical solution, which is obtained only for the bottom of the capsule. However, there is some discrepancy, since melting in the upper part in the analytical solution is neglected. As it was expected a priori this discrepancy does not exceed 15%. Fig. 5 shows the time history of the liquid layer thickness at the bottom of the capsule. According to the numerical solution of the complete model [5,10], at the beginning of melting, the liquid layer thickness rapidly increases, then it has a small peak and after that it continues to grow. The small peak corresponds to the so-called 'Lifting Phenomenon' first pointed out by Saitoh and Moon [13]. This is attributed to the sharp pressure increase at the bottom of the enclosure almost instantly after the beginning of melting. The analytical solution can not catch this early-time effect since the quasi-steady model is assumed. The further trend of liquid layer thickness variation with time is similar for both numerical and analytical solutions. Slightly bigger thickness of the liquid layer in the later period of time obtained numerically is attributed to the lower load exerted by the solid core since its mass is reducing more rapidly due to accounting for melting on the top of the capsule.

## 4. Conclusions

Conclusions drawn are the following:

1. Melting process of the unfixed solid in the spherical capsule was researched both numerically and analytically. In contrast to the previous research our mathematical model for close-contact region accounts for the arbitrary temperature distribution on the capsule's wall and both for heat transport by conduction across the molten layer and convection in the streamwise direction.
2. The approximate analytical solutions of close-contact melting obtained by the perturbations technique are found to be in good agreement with numerical solution of the complete mathematical model. The discrepancy in the results does not exceed 10–15%.
3. Computed results reveal that ignoring the effect of streamwise convection in the liquid layer leads to overestimating of melting rate.
4. The assumption of the constant temperature wall of the capsule, in the previous research can lead to the results which significantly differ from those obtained for the real conditions of melting when the wall of the capsule is non-isothermal.

## References

[1] T.S. Saitoh, K. Hirose, High Rayleigh numbers solutions to problems of latent heat thermal energy storage in a horizontal cylinder capsule, ASME Journal Heat Transfer 104 (1982) 545–553.
[2] K. Katayama, A. Saito, U. Utoka, A. Saito, H. Matsu, H. Maekawa, A. Saiffulah, Heat transfer characteristics of the latent heat thermal energy storage capsule, Solar Energy 27 (1981) 91–97.
[3] M. Bareiss, H. Beer, An analytical solution of the heat transfer process during melting of an unfixed solid phase change material inside a horizontal tube, International Journal of Heat and Mass Transfer 27 (1984) 739–746.
[4] F. Moore, Y. Bayazitoglu, Melting within a spherical enclosure, ASME Journal of Heat Transfer 104 (1982) 19–23.
[5] H. Hoshina, T.S. Saitoh, Numerical simulation on combined close-contact and natural convection melting in thermal energy storage spherical capsule, in: Proceedings of 34th National Heat Transfer Symposium of Japan, Sendai, 1997, pp. 721–722.
[6] P.A. Bahrami, T.G. Wang, Analysis of gravity and conduction-driven melting in a sphere, ASME Journal of Heat Transfer 19 (1987) 806–809.
[7] S.K. Roy, S. Sengupta, The melting process within spherical enclosures, ASME Journal of Heat Transfer 109 (1987) 460–462.
[8] A. Bejan, Single correlation for theoretical contact melting results in various geometries, International Communications in Heat and Mass Transfer 19 (1992) 473–483.
[9] M. Oka, Direct contact melting process on cylindrical heating wall with an arbitrary temperature distribution,

in: Proceedings of the 32nd IECEC Intersociety Energy Conservation Engineering Conference, Honolulu, 1997, vol. 3, pp. 1667–1672.

[10] K. Yamada, Numerical simulation of the latent heat thermal energy storage tank. Master thesis, supervised by T. S. Saitoh, Tohoku University (1997).

[11] M.K. Moallemi, B.W. Webb, R. Viskanta, An experimental and analytical study of close-contact melting, ASME Journal of Heat Transfer 108 (1986) 894–899.

[12] T.S. Saitoh, in: Computer-Aided Heat Transfer, Yokendo, Tokyo, 1986, pp. 116–125.

[13] T.S. Saitoh, J.H. Moon, Experimental performance of latent heat thermal energy storage unit packed with spherical capsules, in: Proceedings of the 5th International Energy Conference, Seoul, 1993, vol. 2, pp. 89–96.